Journal of Modern Optics

Dynamic behaviour in a nonlinear directional coupler with feedback

David Artigas [a]; Federico Dios [a]; Ferran Canal [a]
[a] Department of Signal Theory and Communications, Universitat Politècnica de Catalunya, Barcelona, Spain

PLEASE SCROLL DOWN FOR ARTICLE

Dynamic behaviour in a nonlinear directional coupler with feedback

DAVID ARTIGAS, FEDERICO DIOS and FERRAN CANAL

Universitat Politècnica de Catalunya, Department of Signal Theory and Communications, Gran Capità s/n, Campus Nord, edifici D-3, 08034-Barcelona, Spain

Abstract. A new kind of resonator based on a nonlinear directional coupler with feedback is presented. The steady states are found and the map of the system is iterated, showing the existence of bistability, period doubling and chaos. The dependence of the dynamic features is discussed in terms of the parameters of the two different schemes of feedback studied in this work. A new device based on one of these schemes of feedback suitable as a routing unit is proposed.

1. Introduction

Much attention has been paid to nonlinear resonators due to the variety of physical phenomena they present and the many technological applications that can be derived from them [1]. At first, nonlinear Fabry–Pérot cavities were widely studied [2]. However, ring cavities were proposed in order to study effects of feedback due to the simplicity of analysis [3]. Both versions, loop mirrors [4, 5] and loop fibre [6] ring cavities have been studied theoretically and also experimentally [7]. On the other hand, since the first analysis of nonlinear directional couplers (NLDC) was presented by Jensen [8], this device has become one of the most commonly investigated in the field of optical switching [9–15].

In the present work we analyse a new kind of resonator which combines both of the structures described above. In contrast to the traditional all-fibre ring cavity, the nonlinearity is present in the directional coupler and not in the loop waveguide. As a consequence, the phase, as in ring cavities, as well as the amplitude of the fed back field are intensity dependent. In this case the pump P_{in} is continuous wave (cw) or, if dispersion is not taken into account, synchronized square pulses, i.e. the temporal separation between the pump pulses is equal to the time needed by each of them to make a round trip. Recently, new kinds of oscillators have been proposed based on a similar topology but with a different operational principle. They consist of a nonlinear directional coupler with amplification occurring along the length of the loop waveguide which connects the output port of one channel of the coupler to the input port of the bar channel [16] or of the cross channel [17]. They must be considered as oscillators and not as resonators since they only need an initial single pulse (seed) in the free input port of the nonlinear coupler. In the following round trips the input is in the second port due to amplification. In the first paper on this subject [16], the pulse was taken to be arbitrary, the device being

used to implement a mode-locked fibre laser. The second paper assumed square pulses without taking dispersion into account, with the aim of studying the stability of the configuration [17].

Our device is designed to obtain a new response of the NLDC due to the variations of the initial conditions induced by feedback. In this sense we propose two configurations or schemes for feedback. In the first one, the new response, as in ring cavities, comes from a variation in the input power due to constructive–destructive interferences in a Y junction (also, as in ring cavities, a linear coupler can be used). This configuration presents interesting input–output characteristics: sharp transitions and bistable cycles. However, the usefulness of this configuration is restricted by the presence of period-doubling and chaos. We use this kind of feedback in order to show these effects. The second scheme of feedback is proposed to obtain a new response based on the high sensitivity of the NLDC towards the variation of the excitation (change in the power distribution and/or phase difference in the input ports of the coupler, the total power remaining constant) [13, 14]. The input–output characteristics shown by this last configuration and the fact of having two complementary output ports offers new possibilities. One of these possibilities, discussed here, is the ability to route the signal.

2. Theory

Both proposed configurations of feedback are shown in figure 1. They are based on a NLDC of length L where the media have a Kerr-like nonlinearity defined by

$$n_t^2 = n_i^2 + \alpha |E|^2 \qquad (1)$$

where α is the nonlinear coefficient, n_i the linear refractive index of each layer and n_t is the total index. In the first configuration, just a fraction of the output power is fed back by means of a linear coupler at the output of waveguide 1 into the input of the same waveguide. In the second one, the output of waveguide 2 is fed back into the input port 2. The amplitude transmission coefficient of the linear coupler is K. The loop waveguide of length l_f, is linear and passive. All waveguides are monomode and lossless.

We first present a mapping for the circulating field. We choose to use the supermode technique introduced by Silberberg and Stegeman [10] to model the propagation in the coupler. In this case, the propagation is described by two nonlinear equations for the slowly varying complex amplitudes of the first two TE supermodes $A_i(z) = (P_i(z))^{1/2} \exp(j\phi_i(z))$ where $P_i(z)$ is the power carried by the supermode i and ϕ_i the phase shift due to nonlinearity. This case would be similar to having two modes or to taking two polarizations in a nonlinear ring cavity. The constant propagation of each supermode is β_i. Following [10] we obtain the coupled mode equations in the nth round trip as:

$$\frac{\mathrm{d}}{\mathrm{d}z} U_n(z) = \mathcal{K}P_n C_2 (1 - U_n^2(z)) \sin 2\theta_n(z) \qquad (2)$$

$$\frac{\mathrm{d}}{\mathrm{d}z} \phi_{0,n}(z) = -\mathcal{K}P_n \left(C_0 \frac{1 + U_n(z)}{2} + C_2(1 - U_n(z))(1 + \tfrac{1}{2}\cos 2\theta_n(z)) \right) \qquad (3)$$

$$\frac{\mathrm{d}}{\mathrm{d}z} \phi_{1,n}(z) = -\mathcal{K}P_n \left(C_1 \frac{1 + U_n(z)}{2} + C_2(1 + U_n(z))(1 + \tfrac{1}{2}\cos 2\theta_n(z)) \right) \qquad (4)$$
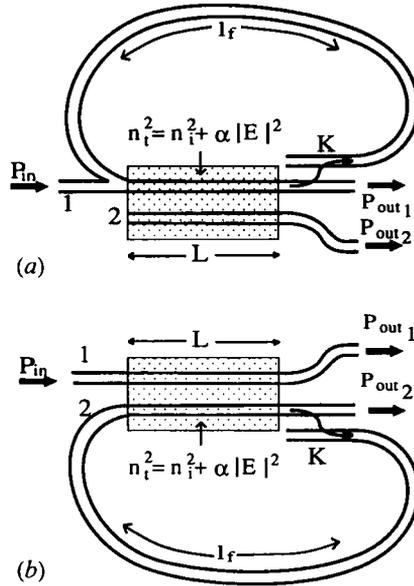
Figure 1. The nonlinear directional coupler with the two schemes of feedback studied in this work.

C_0, C_1 and C_2 being the nonlinear-phase constants defined in [10], $\mathcal{K} = k_0\alpha/4\eta_0$, k_0 being the wavenumber and η_0 the vacuum impedance, P_n the total power inside the NLDC, $U_n(z) = (P_{0,n}(z) - P_{1,n}(z))/P_n$ and $\theta = (\beta_0 - \beta_1)z - (\phi_{0,n}(z) - \phi_{1,n}(z))$. Here, in contrast to [10] where $\theta_n(z)$ is used, the differential equations for the individual nonlinear phase $\phi_{i,n}(z)$ are considered, because both are needed to find the boundary conditions when feedback is present. Equations (2)–(4) are solved using a Runge–Kutta procedure since the analytical solution for the system is known for $U_n(z)$ and $\theta_n(z)$ but not for $\phi_{i,n}$.

2.1. *First configuration*

In the first case (Figure 1 (a)) the loop waveguide is connected to the input port 1 through one branch of an assymetrical Y junction. The pump P_{in} is launched at the other branch of the Y junction. The Y junction is connected to a monomode waveguide, this means that the second mode radiates. Losses in the pump due to radiation can be reduced using an asymmetrical Y junction so that the input field a_1 in waveguide 1 is given by [18]

$$a_1 = b_1 P_{in}^{1/2} + b_2 a_f \tag{5}$$

where a_f is the amplitude of the field that comes from feedback and b_i gives the ratio of the field in the branch i of the Y junction that is converted to the fundamental mode of waveguide 1.

The boundary conditions relate the output of the NLDC at the round trip $n - 1$ with the input at the round trip n throughout the propagation in the linear coupler, the loop waveguide and the Y junction. So, the complex amplitude at the input in waveguide 1, $a_{1,n}(0)$ at the round trip n is related to the amplitude at the output in waveguide 1 $a_{1,n-1}(L)$ using (5) as

$$a_{1,n}(0) = b_1 P_{\text{in}}^{1/2} + b_2 K a_{1,n-1}(L) \exp{(j\varphi)} \tag{6}$$

where the phase shift φ is introduced by the loop waveguide length l_f and the length of the linear coupler. The input in waveguide 2 is always null, which implies that $U_n(0) = 0$ and $\theta_n(0) = \phi_{1,n}(0) - \phi_{2,n}(0) = 0$, but $\phi_{i,n}(0)$ is not necessarily null. Making use of the relations between $A_{i,n}$ and $a_{i,n}$

$$a_{1,n}(z) = \frac{1}{2^{1/2}} (A_{0,n}(z) + A_{1,n}(z))$$

$$a_{2,n}(z) = \frac{1}{2^{1/2}} (A_{0,n}(z) + A_{1,n}(z)) \tag{7}$$

which hold for sufficiently separated waveguides, the expression (6) can be written in terms of the variables of the coupler. Then the boundary conditions for the internal power in the NLDC, P_n, and $\phi_{i,n}(0)$ are given by

$$P_n = b_1^2 P_{\text{in}} + \frac{b_2^2 K^2 P_{n-1}}{2} (1 - (1 - U_{n-1}^2(L))^{1/2} \cos{\theta(L)})$$

$$+ b_1 b_2 K (P_{\text{in}} P_{n-1})^{1/2} ((1 - U_{n-1}(L))^{1/2} \cos{(\beta_1 L - \phi_{1,n-1}(L) - \varphi)}$$

$$+ (1 + U_{n-1}(L))^{1/2} \cos{(\beta_0 L - \phi_{0,n-1}(0) - \varphi)}) \tag{8}$$

$$\phi_{i,n}(0) = \arcsin{\left[b_2 K \left(\frac{P_{n-1}}{4 P_n} \right)^{1/2} ((1 - U_{n-1}(L))^{1/2} \sin{(\beta_1 L - \phi_{1,n-1}(L) - \varphi)} \right.}$$

$$\left. - (1 + U_{n-1}(L))^{1/2} \sin{(\beta_0 L - \phi_{0,n-1}(L) - \varphi)} \right] \tag{9}$$

2.2. *Second configuration*

In this case (figure 1 (*b*)) the complex amplitude at the input in waveguide 2, $a_{2,n}(0)$ at the n round trip, is related to the amplitude at the output in waveguide 2, $a_{2,n-1}(L)$ by the boundary condition

$$a_{2,n}(0) = K a_{2,n-1}(L) \exp{(j\varphi)} \tag{10}$$

where the phase change φ depends on l_f and the length of the linear coupler. The input in waveguide 1 is always

$$a_{1,n}(0) = P_{\text{in}}^{1/2} \tag{11}$$

where we have considered a null initial phase. However (10) and (11) do not relate the initial condition P_n, $U_n(0)$ and $\phi_{i,n}(0)$ and P_{n-1}, $U_{n-1}(L)$ and $\phi_{i,n-1}(L)$. Using (7), the boundary condition (10)–(11), can be written as

$$P_n = P_{\text{in}} + \tfrac{1}{2} K^2 P_{n-1} (1 - (1 - U_{n-1}^2(L))^{1/2} \cos{\theta(L)}) \tag{12}$$

$$U_n(0) = \frac{\sqrt{P_{\text{in}} P_{n-1}}}{P_n} K ((1 + U_{n-1}(L))^{1/2} \cos{(\beta_0 L - \phi_{0,n-1} - \varphi)}$$

$$- ((1 - U_{n-1}(L))^{1/2} \cos{(\beta_1 L - \phi_{1,n-1} - \varphi)}) \tag{13}$$

$$\phi_{i,n}(0) = \arcsin\left[(-1)^i K\left(\frac{P_{n-1}}{2P_n(1 + U_n(0))}\right)^{1/2}\right.$$

$$\times ((1 - U_{n-1}(L))^{1/2} \sin(\beta_1 L - \phi_{1,n-1} - \varphi)$$

$$\left. - (1 + U_{n-1}(L))^{1/2} \sin(\beta_0 L - \phi_{0,n-1} - \varphi))\right] \qquad (14)$$

3. Discussion

Equations (2)–(4) and the boundary condition (8)–(9) in the first configuration, and (12)–(14) in the second one, define the map to be iterated. The parameters that affect the device behaviour are the phase shift φ introduced by the loop waveguide, the coefficients K, and L/L_c. The last parameter specifies the contribution of the NLDC, L_c being the linear half beat length.

Figure 2 shows the input–output characteristic for the half beat length NLDC ($L/L_c = 1$) in both cases, without feedback (dashed lines) and in the first configuration presented in this work (solid lines). The figure is obtained for the steady state case, i.e. the solution of the map taking $n = n - 1$. The plot is for a configuration whose parameters are: $\varphi = \pi$, $K = 0.3$, and $b_1 = 0.92$ and $b_2 = 0.3$. Moreover, power in all plots is normalized with respect to the NLDC critical power. This figure shows a very sharp switch characteristic at an input power of $P_{in} = 1.15P_c$ and a bistable cycle at $2.1P_c < P_{in} < 2.4P_c$. The mechanism causing the change of the input–output characteristic is the change of the internal power in the coupler due to constructive–destructive interference in the Y junction. This mechanism only acts when feedback is significant, that is, at powers near and above the critical one.

Figure 3 has been obtained iterating the map until the output reaches a stationary state. The P_{in} is increased and the map is again iterated. When P_{in} is
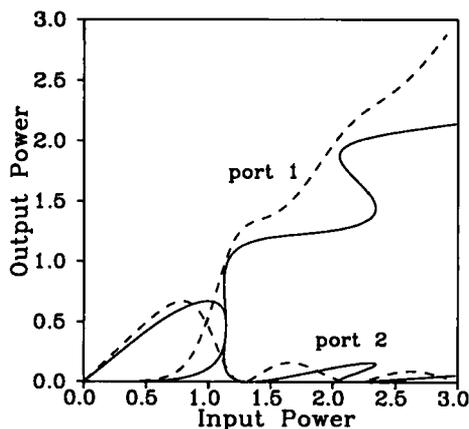

Figure 2.   Input-output characteristic of a half-beat length NLDC (dashed lines) and of a NLDC with the feedback shown in figure 1 (*a*) in the stationary state (solid lines). Labels indicate the output port.
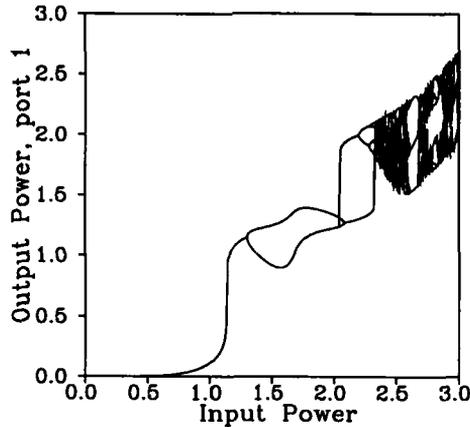
Figure 3.   Port 1 input–output characteristic of first scheme. In this case we use a half-beat length NLDC and the map is iterated.

high enough, the procedure is inverted, and P_{in} is decreased progressively. The input–output characteristic in figure 2 could be useful to develop all-optical memory units or switching elements. Unfortunately, the iteration of the map shows that not all the stationary states are stable. If a steady state is unstable, it does not appear when the map is iterated. Thus, we can distinguish two possible situations. First, one of the three outputs for each bistable cycle in figure 2 is unstable. These unstable states are those that satisfy $dP_n/dP_{in} < 0$ for the stationary case [4]. These points do not appear in figure 3, the vertical straight lines being the jumps between the lower and the upper branches of the bistable cycles. The second case is due to Ikeda-like instabilities, that is, the existence of period doubling (P2) and chaos at the coupler output ports. In figure 3 the bifurcation points are clearly appreciated, the first of them appearing just after the sharp transition. In this case the output in port 1 oscillates alternatively at each round trip between the two powers plotted in figure 3. A succession of P2 can lead to a chaotic behaviour. The route to chaos is plotted at input powers above $2 \cdot 2 P_c$. Figure 4 shows the rsults of the simulation for the output power evolution in terms of the round trip n for some particular input power. Figure 4(a) shows the evolution toward period-two state reached at $P_{in} = 1 \cdot 5 P_c$. Figure 4(b), 4(c) and 4(d) show respectively the period-four state at $P_{in} = 2 \cdot 3 P_c$, chaotic behaviour at $P_{in} = 2 \cdot 5$ and the output of the period-three window that can be observed at $P_{in} = 2 \cdot 69$.

The dynamic shown by figures 2 and 3 depends on the values of the parameters. The position of the bistable cycles, which are always present above $P_{in} = 1 \cdot 2 P_c$, depends on the value of φ. This one is the most critical parameter. A 2π variation of this parameter means that the variation of total length is only λ. The relevance of such length sensitivity for practical implementations is commented on later. Concerning the remaining parameters, an increment of K or of the NLDC length, implies that the effects of the nonlinearity are more important, leading to the existence of chaos at lower input powers.
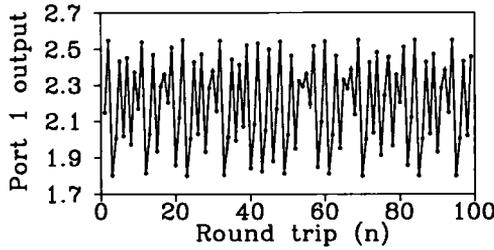
The potential of using the input–output characteristic this first configuration presents is limited by the existence of chaotic dynamics. If $L \simeq L_c$ and $K < 0 \cdot 3$, it is possible to take advantage of the bistable cycles without the presence of chaos.
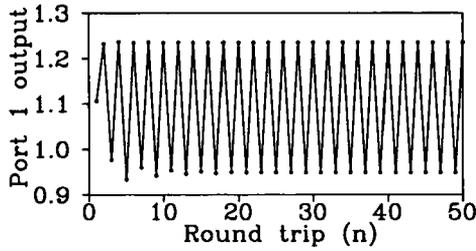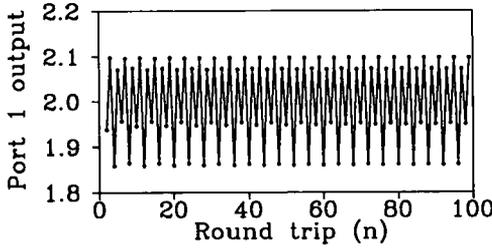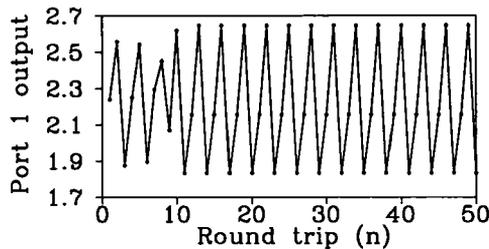
Figure 4. Detail of output power of figure 3 as a function of the number of round trips n for four different input powers: (*a*) period-two at $P_{in} = 1.5P_c$, (*b*) period-four at $P_{in} = 2.3P_c$, (*c*) chaos in $P_{in} = 2.5P_c$ and (*d*) period-three at $P_{in} = 2.69P_c$.

The input–output charcteristic of the second configuration (figure 1 (*b*)) is plotted in figure 5 for two different lengths of the coupler, using the same values for the parameters that were taken in the previous configuration. In this case the plots correspond to the iteration of the map. The fact of iterating the map instead of finding the steady output only causes a loss of information about the unstable
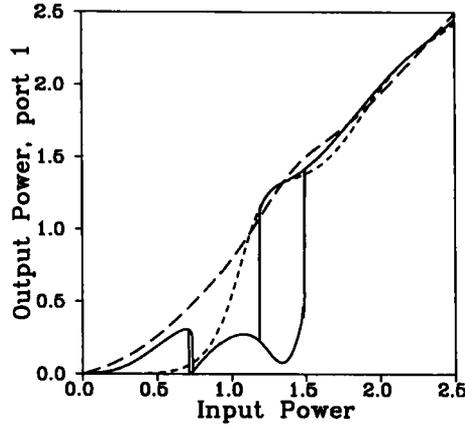
Figure 5.   Port 1 input-output characteristic for the half-beat NLDC in the case of the second scheme of feedback (solid lines $\varphi = \pi$) and in the case where $\varphi = 0$ (long-dashed lines). Short-dashed lines correspond to the NLDC without feedback.

branch of the bistable cycles. The first difference in relation to the previous configuration is the range of input powers at which feedback acts. In this configuration there is feedback at powers below and near the critical power, so, contrarily to the previous case, the most interesting feature occurs at low powers. The second difference is the mechanism underlying the device behaviour. Opposite to the previous configuration and ring cavities, where the working effect is interference, in the second configuration, that mechanism corresponds to changes in the excitation $(U(0), \theta(0))$ [13, 14]. The solid line in figure 5 shows the port 1 output for a coupler length $L = L_c$, this being one of the cases showing bistability. Bistability has been also obtained for lengths between $0 \cdot 9 L_c$ and $1 \cdot 2 L_c$. The long-dashed line in figure 5 corresponds to a small change in the length of the coupler or in the loop waveguide which is equivalent to a value $\varphi = 0$ showing the extreme sensitivity of the behaviour toward the dimensions of the waveguides. The bistable cycle has been obtained for a range of $3/4\pi < \varphi < 3/2\pi$ (a variation of the length of $3/8\lambda$). At $K > 0 \cdot 4$ the configuration presents bifurcations and chaos near the critical power.

The main advantage of the present device comes from the two complementary output ports, which allow more versatility to this new resonator. One possibility in order to take advantage of the bistable cycle shown in figure 5 and the two output ports, is to use the NLDC with this second scheme of feedback to route the signal. The transition from the low to the high state in the bistable cycle, which is equivalent to a switch from the lower to the upper branch of the NLDC, can be obtained by increasing the input power above $P_{in} \gg 1 \cdot 5 P_c$ (positive trigger) in just one round trip. The opposite transition is obtained by decreasing the input power below $P_{in} \ll 1 \cdot 19 P_c$ (negative trigger). The output power in both branches has been plotted in figure 6 as a function of the number of round trips. At the round trip $n = 100$ a positive trigger has been added $(P_{in} = 2 P_c)$ whereas for $n = 200$ the trigger was negative $(P_{in} = 0 \cdot 4 P_c)$, showing the switch between branches. As a consequence, a signal previously routed to an output port, would remain in the selected port until a new trigger would be launched. Then, as figure 6 shows, the signal would be routed to the opposite branch.
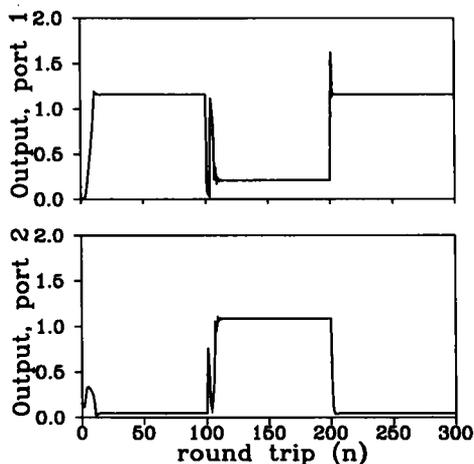
Figure 6.   Output power of the second scheme of feedback as a function of the number of round trips n for an input power $P_{in} = 1.3P_c$. At $n = 100$ a positive trigger has been added and at $n = 200$ a negative one.

The bistable cycle shown in figure 5 makes this configuration suitable to be used as an all-optical memory unit. This use of bistable cycles is also common in other resonators. However, when compared to a ring cavity, our device, used as a memory unit, does not present any relevant advantage.

The main drawback of the experimental study and practical implementation, as in all resonators, is the critical dependence of the behaviour on the length. The length is affected by two factors: (a) the accuracy in the implementation and (b) the variations in the optical path due to ambient variations. The second one is less important if the device is completely integrated using AlGaAs technologies [15]. However, in this case the problem is the tolerance in the dimensions, more progress is AlGaAs technologies being necessary. In contrast, if the device is implementary using an optical fibre, the change in the ambient conditions is precisely the main problem. This case requires an interferometric stabilization of the fibre loop, which nowadays is possible to reach with an accuracy of $\lambda/200$ [19]. The bistable cycle appears in a range of length $\Delta L = 3/8\lambda$, so he precision offered by this technique is excellent. Moreover, using this method of controlling the optical path, the problem of accuracy in the dimensions of the components of the resonator can be counter-worked.

Other configurations, which consist in connecting output port 1 with the input port 2, and in connecting output port 2 with input port 1 have also been studied. The first case presents chaotic dynamics at very low feedback values ($K < 0.1$). In the second case it has only been possible to obtain a bistable cycle connecting directly the output port 2 with the input port 1. Therefore, as the device only has one output, it loses all the advantages with respect to ring cavities.

4. Conclusions

In this paper we have presented a preliminary study of a new kind of nonlinear resonator where the nonlinearity is originated from the inclusion of a nonlinear

directional coupler. This means, that contrarily to the well known nonlinear ring cavities, this device allows one to obtain two different output ports which coincide with the branches of the NLDC. In the first scheme of feedback presented, feedback acts when the input power is above the critical power of the NLDC, showing bistability, period doubling and chaos. This behaviour is caused by the change of the power at the input of the NLDC due to constructive–destructive interferences in a Y junction. The half-beat length coupler shows the most interesting input–output characteristic due to the possibility of obtaining bistable cycles without the presence of chaos at powers near the critical one. In the second scheme, feedback acts at input powers below the critical one. The dynamics of this configuration are a consequence of the change in the excitation due to feedback. This configuration shows bistable cycles at input powers near the critical one. Based on a bistable cycle, and taking advantage of the two output ports offered by the resonators, this device is proposed as a means of routing the signal.

References

[1] GIBBS, H. M., 1985, *Optical Bistability: Controlling Light with Light* (London: Academic Press), chap. 2.
[2] FELBER, F. S., and MARBURGER, J. H., 1976, *Appl. Phys. Lett.*, **28**, 731.
[3] BONIFACIO, R., and LUGIATO, L. A., 1978, *Lett. Nuovo Cimento*, **21**, 505.
[4] IKEDA, K., 1979, *Optics Commun.*, **30**, 257.
[5] IKEDA, K., DAIDO, H., and OKIMOTO, O., 1980, *Phys. Rev. Lett.*, **45**, 709.
[6] HAELTERMAN, M., 1993, *Optics Commun.*, **100**, 389.
[7] VALLÉE., R., 1991, *Optics Commun.*, **81**, 419.
[8] JENSEN, S. M., 1982, *IEEE J. Quantum Electron.*, **18**, 1580.
[9] STEGEMAN, G. I., WRIGHT, E. M., FINLAYSON, N., ZANONI, R., and SEATON, C. T., 1988, *J. Lightwave Technol.*, **6**, 953; STEGEMAN, G. I., and WRIGHT, E. M., 1990, *J. Opt. Quantum Electron.*, **22**, 95.
[10] SILBERBERG, Y., and STEGEMAN, G. I., 1987, *Appl. Phys. Lett.*, **50**, 801.
[11] THYLEN, L., WRIGHT, E. M., STEGEMAN, G. I., SEATON, C. T., and MOLONEY, J. V., *Opt. Lett.*, **11**, 739.
[12] SNYDER, A. W., MITCHELL, D. J., POLADIAN, L., ROWLAND, D. R., and CHEN, Y., 1991, *J. opt. Soc. Am.* B, **8**, 2102.
[13] WABNITZ, S., WRIGHT, E. M., SEATON, C. T., and STEGEMAN, G. I., 1986, *Appl. Phys. Lett.*, **49**, 838.
[14] ARTIGAS, D., and DIOS, F., 1994, *IEEE J. Quantum Electron.*, **30**, 1587.
[15] STEGEMAN, G. I., VILLANEUVE, A., KANG, J., AITCHINSON, J. S., IRONSIDE, C. N., AL-HEM-YARI, K., YANG, C. C., LIN, C. H., KENNEDY, G. T., GRANT, R. S., and SIBBETT, W., 1994, *Int. J. Nonlinear opt. Phys.*, **3**, 347.
[16] LANGRIDSGE, P. E., and FIRTH, W. J., 1995, *Optics Commun.*, **86**, 170.
[17] KARPIERZ, M. A., KUJAWSKI, A., and SZCZEPANSKI, P., 1995, *J. mod. Optics*, **42**, 1079.
[18] BURNS, W. K., and MILTON, A. F., 1975, *IEEE J. Quantum Electron.*, **11**, 32.
[19] REYNAUD, F., and DELAIRE, E., *Electron. Lett.*, **29**, 1718.